

Modified Transformer-Less Single Switch High Voltage Gain Boost Converter

Ijas Mohammed,

PG Scholar Dept of Electrical & Electronics Engg,
Mar Athanasius College of Engineering
Kothamangalam, Kerala

Kavitha Issac

Dept of Electrical & Electronics Engg,
Mar Athanasius College of Engineering
Kothamangalam, Kerala

Anu George

Dept of Electrical & Electronics Engg,
Mar Athanasius College of Engineering
Kothamangalam, Kerala

Geethu James

Dept of Electrical & Electronics Engg,
Mar Athanasius College of Engineering
Kothamangalam, Kerala

Abstract:- The transformer-less single-switch dual-inductor boost converter configuration can realize high voltage gain with low voltage and current stresses; therefore, it is suitable for high gain applications. It has low voltage stress on components compared to other typical transformer-less single-switch high voltage gain converters like switched inductor boost converter, quadratic boost converter and quasi-Z-source boost converter. Moreover, the current stress of the front-end diode and the rear-end inductor is also relatively low. Therefore, the conversion efficiency is enhanced while keeping the cost low. The operation principles and steady-state characteristics analysis of the converter is discussed in detail. Results are obtained by simulating the converter in MATLAB/SIMULINK R2021b. The simulation results show that the converter has high voltage gain and achieves a peak efficiency of 89%. The converter is controlled using TMS320F28335 microcontroller. The experimental results obtained from a 6W converter prototype confirm the theoretical considerations and the simulation results.

Keywords:- Boost Converter, Transformerless, Gain, Efficiency.

I. INTRODUCTION

As the global energy demand is escalating, renewable energy systems are becoming more popular as they meet the demand while keeping the environment eco-friendly and sustainable [5]. Generally, renewable energy sources such as solar photovoltaic (PV) and fuel-cell produce a low and variable dc output voltage. Thus, dc-dc step-up converters with sufficient voltage gain are usually required to meet the load or grid voltage requirements [3]. The conventional boost converter is of the most widely adopted converters for step-up applications due to simple structure, continuous input current, ease of control and low cost. Theoretically, the ideal voltage gain of boost converter can tend to infinity; however, the inductor winding resistance limits the maximum practical voltage gain. Moreover, the high voltage gain can only be achieved by applying the duty cycle close to one. In this situation, the current stress significantly increases, and the component non-idealities such as

semiconductor forward voltage drops and diode reverse recovery lead to significant power losses.

Therefore, the efficiency decreases dramatically at high duty cycle operation [4].

In order to overcome the limitations imposed by the boost converter, several high-gain dc-dc converters utilizing various voltage boosting techniques have been proposed. One group of the converters is classified as the transformer-less high voltage gain converters. There are many high voltage gain topologies evolved from three typical transformer-less single-switch dual-inductor topologies, including, switched inductor boost converter, quadratic boost converter and quasi-Z-source boost converter. The switched inductor boost converter can realize high voltage gain and is suitable for high step-up applications. However, switched inductor boost converter has several drawbacks, such as more diodes (four) and considerable input current fluctuation, which can result in noticeable EMI. Moreover, the voltage stress on the power switches is substantially high. The quadratic boost converter is derived by sharing the switches of cascaded boost converters and adding an additional blocking diode. Consequently, its voltage gain is expressed by a quadratic function in terms of the voltage gain of conventional boost converter, and it can easily realize high conversion ratio without extremely high duty cycle operation. However, the voltage stress on the switch and the rear-end diode is still equal to the output voltage. In order to realize the high voltage gain, a quasi-Z-source network is integrated into the boost converter. The quasi-Z-source boost converter employs the fewest diodes compared to the quadratic and the switched inductor topologies, but their maximum duty cycle cannot exceed 0.5. Thus, the conversion efficiency is difficult to improve at low duty cycle operation. Also, the voltage gain is sensitive to the change in duty cycle, and the slope of the gain curve is large, which increases the control complexity. Besides, both the inductor and the diode in the quasi-Z-source network suffer from high current stress. Furthermore, the issue of high voltage stress is still retained, which limits the further optimization of efficiency and cost.

In order to address the aforementioned issues, a transformer-less single-switch dual-inductor high voltage gain boost converter is presented. It is constructed by introducing an intermediate capacitor CZ with the diode of the conventional boost converter, and integrating a charging circuit consisting of an inductor, capacitor and diode. Also, a voltage multiplier circuit is introduced between the input and output which increases the voltage gain. The voltage stress on the switch and the rear-end diode and the average current stress through rear-end inductor and front-end diode are significantly reduced compared to other typical dual-inductor high-gain boost converters. Therefore, the proposed converter reduces the cost and improves the voltage gain.

II. METHODOLOGY

The modified transformer-less high gain boost converter consists of single switch (S), four diodes (D1, D2, D3 and D4), two inductors (L1 and L2) and five capacitors (C1, CZ, C2, C3 and Co). Figure 3.6 shows the Modified transformer-less high gain boost converter.

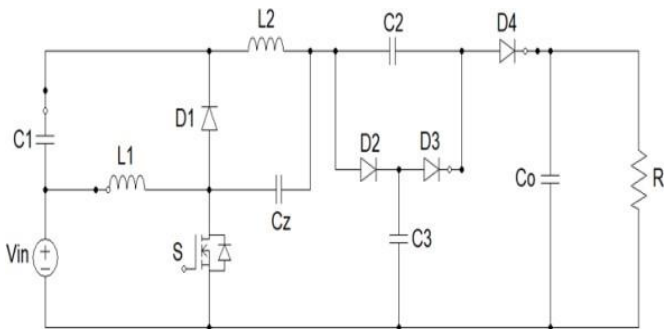


Fig 1:- Transformer-less Boost Converter

A. Modes of Operation

The proposed boost converter has two main operation modes: Continuous conduction mode (CCM) and Continuous bidirectional conduction mode (CBCM). In both modes, the input inductor current i_{L1} continuously flows in one direction. The difference between the operation in CCM and CBCM is that the rear-inductor current i_{L2} flows continuously in a unidirectional and bidirectional fashion in CCM and CBCM, respectively.

1) *Mode 1:* At $t = t_0$, when switch S is turned ON, diodes D1, D2 and D4 are reversed biased. The input inductor L1 is being charged by the input voltage source V_{in} , while the rear-end inductor L2 and the intermediate capacitor CZ are charged by C1 and V_{in} . C3 charges C2 and CZ. Therefore, the output filter capacitor C_o delivers energy to the load. Figure 2 shows operating circuit of mode 1.

Mode 2: At $t = t_1$, when switch S is turned OFF, diodes D1 and D2 conduct and become forward biased. A part of the energy stored in L1 transfer to C1 and the remaining goes to C_o and load. The stored energy in L2 directly transfers to the output side. The intermediate capacitor CZ discharges in this state. Figure 3 shows the operating circuit of mode 2.

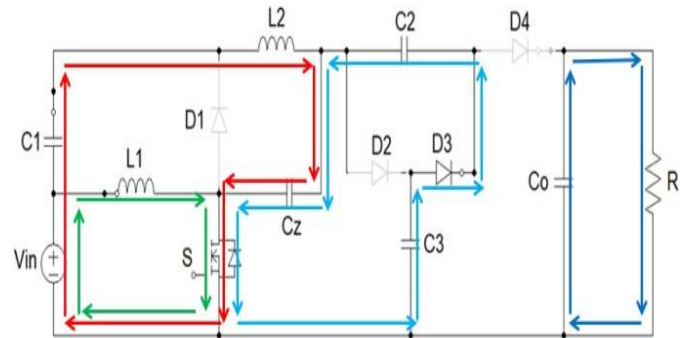


Fig 2:- Operating circuit of of Mode 1

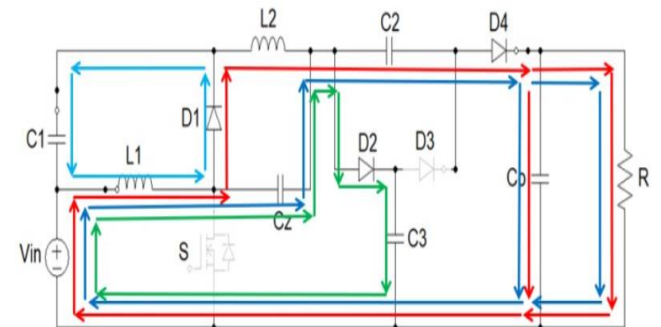


Fig 3:- Operating circuit of of Mode 2

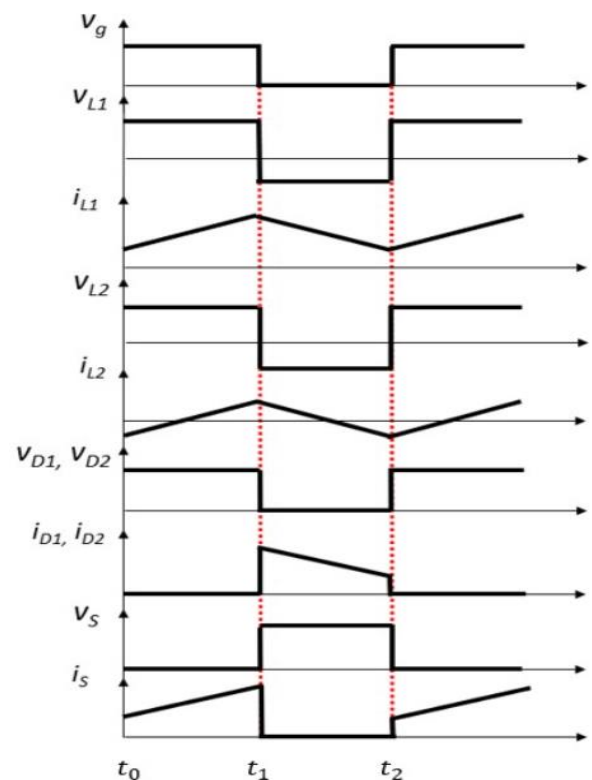


Fig 4:- Theoretical waveform

B. Design of Components

The input voltage is taken as $V_{in} = 48V$. The output power and output voltage are taken as $P_o = 590W$ and $V_o = 462V$. Switching frequency, $f_s = 100kHz$, so time period, $T_s = 1/f_s = 0.00001sec$.

Load resistance can be found by the equation,
Duty ratio,
 $R_o = V_o^2$

$$\frac{P_o}{462^2} = 590 = 360\Omega \quad (1)$$

Figure 4 shows the theoretical waveforms for mode 1 and mode 2.

$$D = \frac{V_o - V_{in}}{V_o + V_{in}} = \frac{300 - 48}{300 + 48} = 0.728 \quad (2)$$

The inductors L_1 & L_2 are obtained from the following equations.

$$L_{L1} = I_o * \frac{1 + D}{1 - D} = 0.83 * \frac{1 + 0.728}{1 - 0.728} = 5.3A \quad (3)$$

$$LI > \frac{V_{in}DT_s}{0.2I_{L1}} \quad (4)$$

It is approximated to 2 mH.

$$I_{L2} = 0.83A = I_o \quad (5)$$

$$L2 < \frac{V_{in}DT_s}{2I_{L2}} \quad (6)$$

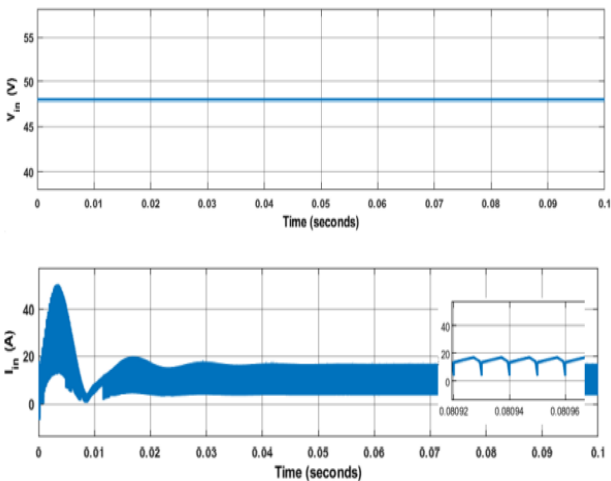


Fig 5:- (a) Input Voltage (V_{in}) and (b) Input Current (I_{in})

The value is chosen to be $100\mu H$.

Capacitors values are found from the following equations.
 $I_o T_s D^2$

$$C_1 \geq$$

$$C_Z \geq$$

$$\frac{0.01V_{in}(1 - D)}{I_o T_s D^2}$$

$$I_o T_s D^2$$

$$\frac{0.01V_{in}(1 - D)}{I_o T_s D^2}$$

$$(7)$$

$$(8)$$

C_1 and C_Z is taken as $20\mu F$

$$C_2 \geq$$

$$I_o T_s D^2$$

$$(9)$$

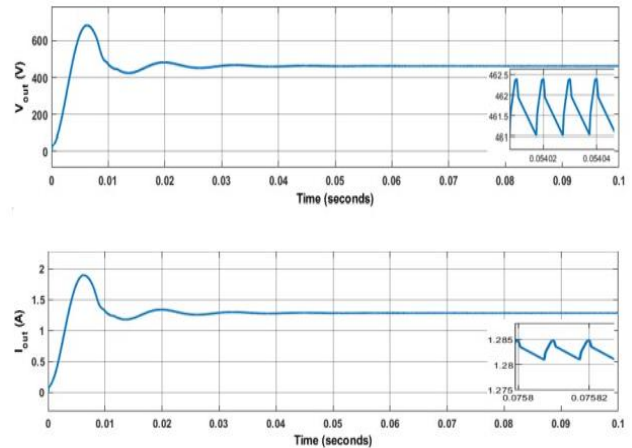


Fig. 6. (a) Output Voltage (V_o) and (b) Output Current (I_o)

$$0.01V_o(1 - D)$$

$$I_o T_s D^2$$

the voltage across the diodes. It can be seen that the voltage

$$C_3 \geq 0.01V$$

$$(10)$$

$$V_o(1 - D)$$

across diodes D1 and D2 are the same which is 176V.

$$C_o \geq$$

$$I_o T_s D^2$$

$$\frac{0.01V_o(1 - D)}{I_o T_s D^2}$$

$$(11)$$

C_2 , C_3 and C_o are taken as $10\mu F$

III. SIMULATIONS AND RESULTS

The transformer-less boost converter is simulated in MAT-LAB/SIMULINK by choosing the parameters listed in Table

1. The switch is MOSFET with constant switching frequency of 100 kHz. A dc input voltage, V_{in} of 48V gives a dc output

Parameters	Value
Input voltage, V_{in}	48V
Output voltage, V_o	462 V
Switching frequency, f_s	100 kHz
Rated power, P_o	593 W
Inductance, L_1	2 mH
Inductance, L_2	100 μ H
Capacitance, C_1, C_2	20 μ F
Capacitance, C_2, C_3, C_o	10 μ F

Table 1 Simulation Parameters of Transformerless Boost Converter

voltage, V_o of 462V for an output power, P_o of 590W. Fig. 5 shows the input voltage and current, Fig. 6 shows the output voltage and current. Thus, the voltage gain is obtained as 9.6.

Fig. 7 shows the gate pulse and voltage stress across the switch. Voltage stress across the switch is 173 V. Fig. 8 shows

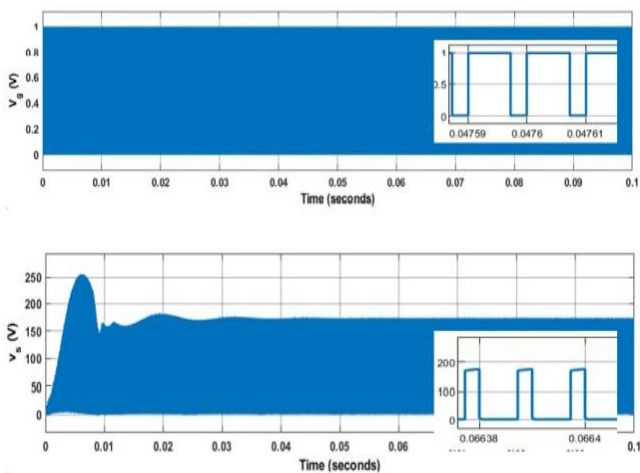


Fig. 7. Gate Pulse (V_g) and Voltage Stress (V_s) of switch S

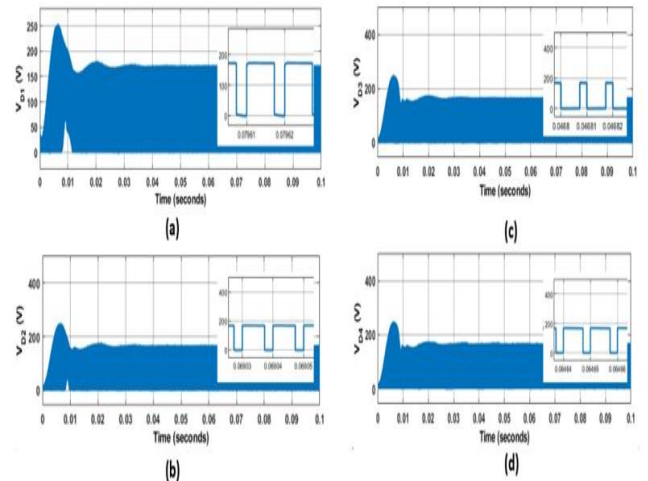


Fig. 8. (a) Voltage across diode (D1) (b) Voltage across diode (D2) (c) Voltage across diode (D3) (d) Voltage across diode (D4)

The voltage across capacitors is obtained as $V_{C1} = 125$ V,

$V_{C2} = 124$ V, $V_{C3} = 166$ V, $V_{C4} = 297$ V, & $V_{C5} = 462$

V which is shown in Fig 8. Fig. 9 shows the current across inductances L_1 and L_2 . It can be seen that the current across filter inductances i_{L1} is 13.7A, i_{L2} is 0.4A.

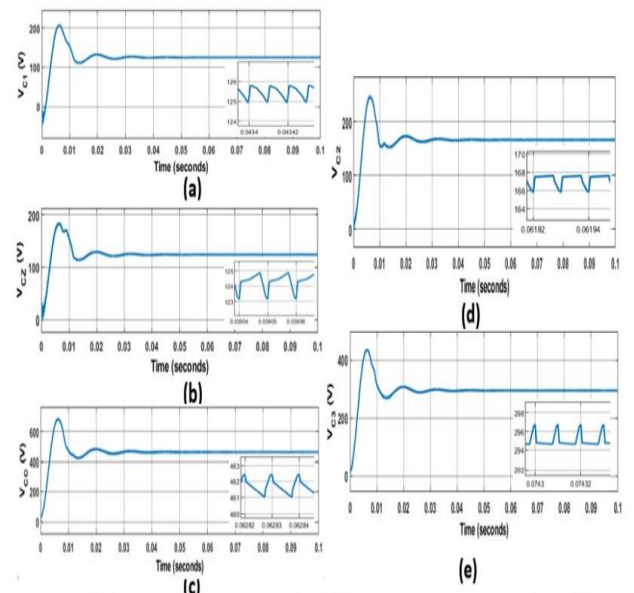


Fig. 9. Voltage across Capacitor (a) V_{C1} , (b) V_{C2} , (c) V_{C3} , (d) V_{C4} , (e) V_{C5}

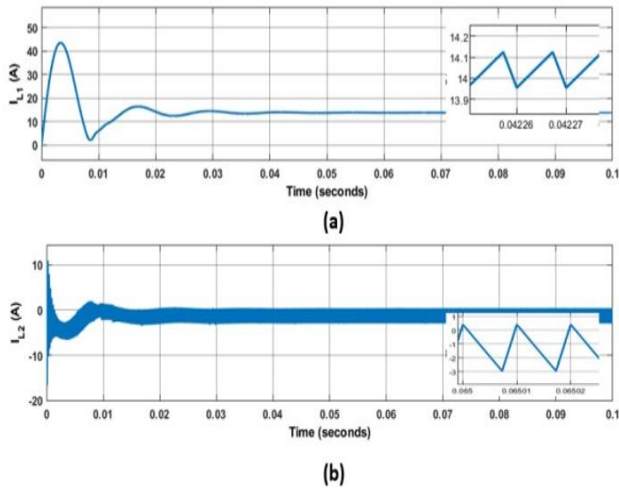


Fig. 10. Current across Inductance (a) i_{L1} , (b) i_{L2}

IV. PERFORMANCE ANALYSIS

Efficiency of a power equipment is defined at any load as the ratio of the power output to the power input. Here the efficiency Vs output power with R load and RL load for transformerless boost converter is done and shown in Fig. 11. The maximum converter efficiency for R & RL load are obtained as 89% and 90.4% . The variation of efficiency with power output is medium for both load ie about 590 W. Thus, the transformerless boost converter can be used in medium power applications.

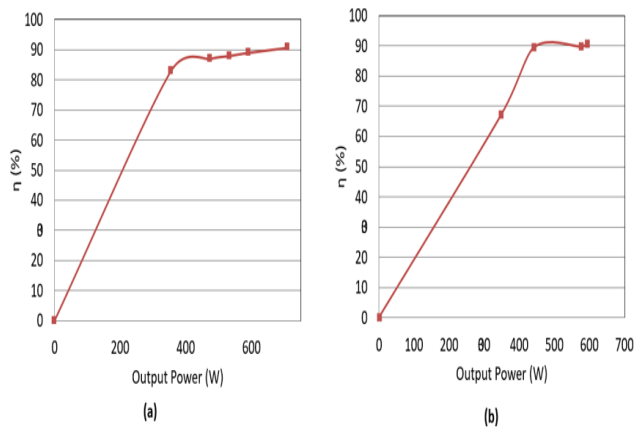


Fig. 11. Efficiency Vs Output Power for (a) R load (b) RL load

The plot of gain of transformer-less boost converter as a function of duty ratio is shown in figure 12. The gain increases as the duty ratio is varied.

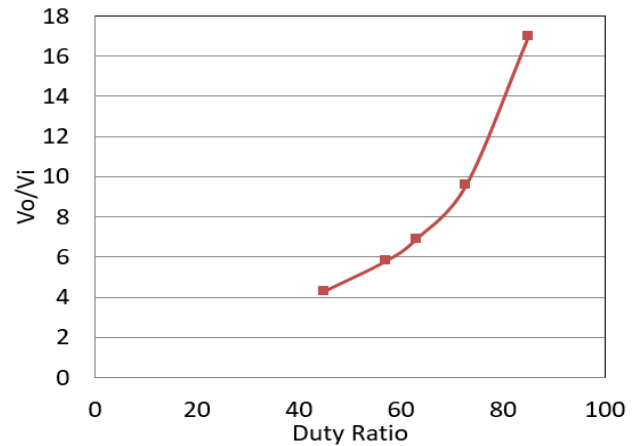


Fig. 12. Voltage gain VS Duty ratio

The plot of output voltage ripple as a function of duty Ratio for transformerless boost converter is shown in figure 13.

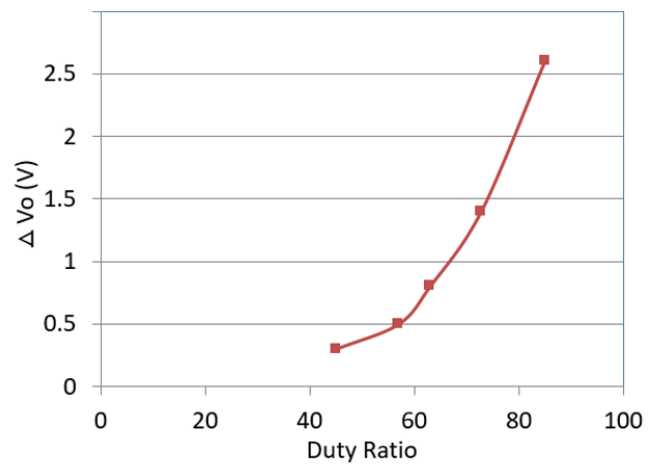


Fig. 13. Output Voltage Ripple VS Duty Ratio

The plot of output voltage ripple as a function of Switching Frequency for modified boost converter is shown in figure 14. The output voltage ripple is decreased as the switching frequency is increased.

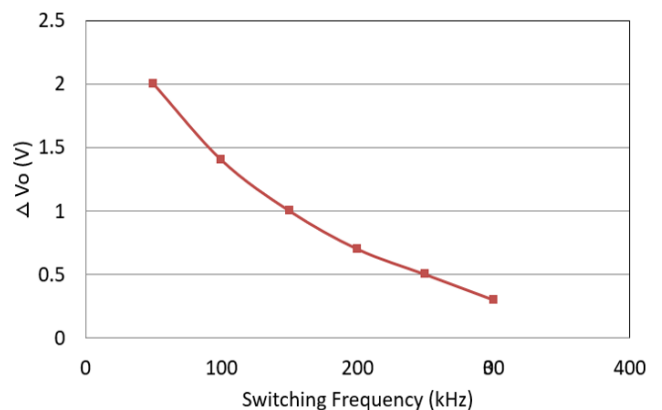


Fig. 14. Output voltage ripple VS frequency

V. COMPARATIVE STUDY

The comparison between a transformer less boost converter with same input voltage and switching frequency & the proposed transformer less boost converter is given in table 2. On the comparison it can be observed that, with same values for input voltage as 48V & switching frequency as 100kHz, the gain is increased from 6.35 to 9.6. But, output voltage and current ripple is more in proposed converter.

Parameters	Transformer less Boost Converter	Proposed Transformer less Boost Converter
No. of switches	1	1
No. of inductor	2	2
No. of capacitor	3	5
Voltage gain	6.35	9.6
Efficiency	92.38%	89%
Output Voltage Ripple	0.35 V	1.4 V
Output Current Ripple	0.0005 A	0.005 A
Voltage Stress across Switch	$3.7V_{in}$	$3.6V_{in}$

Table 2 Comparison Between Transformerless Boost Converters & Proposed Transformerless Boost Converter

Table 3 shows the component wise comparison between proposed transformerless boost converter and other converters. Comparison is based on the components used in the different converters.

Converters	Proposed Transformer less Boost Converter	Switched inductor Boost converter	Quadratic boost converter	Quasi-Z-source boost converter
Switches	1	1	1	1
Inductors	2	2	2	2
Capacitors	5	1	2	3
Diode	4	4	3	2

Table 3 Comparison Between Transformerless Boost Converter & Other Converters

VI. EXPERIMENTAL SETUP WITH RESULT

For the purpose of implementing hardware, the input voltage is reduced to 5V and the switching pulses are generated using TMS320F28335 processor. The switch used is MOS- FET IRF3205. Driver circuit is implemented using TLP250H, which is an optocoupler used to isolate and protect the microcontroller from any damage and also to provide required gating to turn on the switches.

Experimental setup of transformerless boost converter is shown in Fig. 15. Input 5V with 1.4A DC supply is given from DC source. Switching pulses are taken from TMS320F28335 microcontroller to driver circuit. Thus, an output voltage of 45V is obtained from power circuit that is shown in Fig. 16. Output voltage of converter is taken from the DSO oscilloscope.

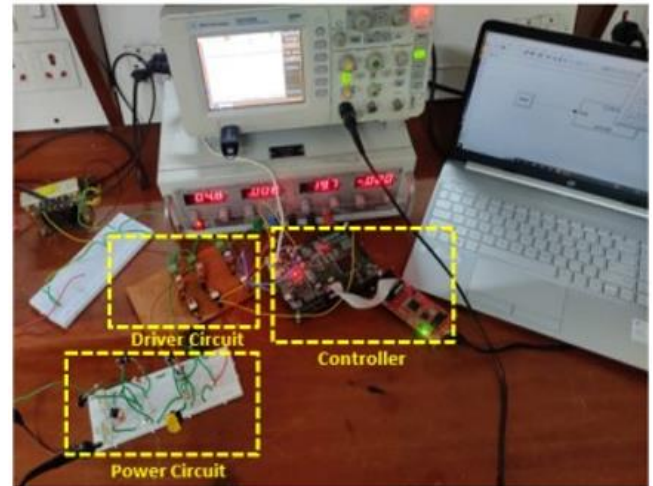


Fig. 15. Experimental Setup

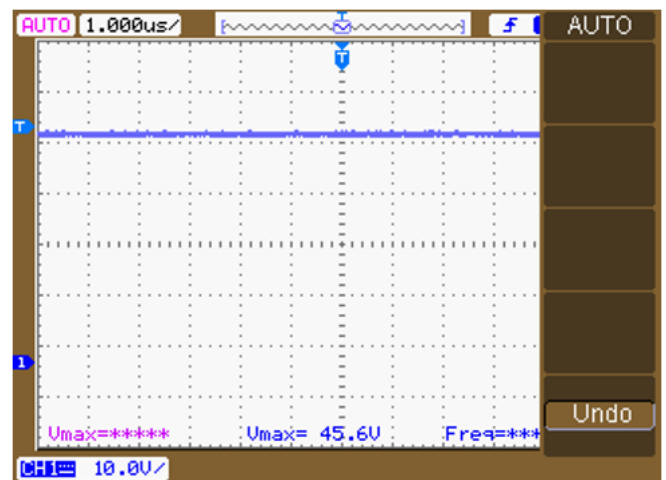


Fig. 16. Output Voltage of Proposed Converter

VII. CONCLUSION

The transformerless boost converter proposed can realize a high voltage gain with low voltage and current stresses. The gain is improved by using a voltage multiplier circuit. However, this resulted in a slight decrease in efficiency as the component count is increased. The operation principles and the steady-state characteristics, including voltage gain, voltage stress, and average current stress in both CCM and CBCM, are the same. A lower value of inductance for L2 is selected to operate the proposed converters in CBCM, which reduces the converter size and cost. The proposed converter has relatively higher efficiency in CBCM than CCM. The efficiency obtained is nearly 89%. The control of the proposed converter is implemented using TMS320F28335 microcontroller. Converter prototype of 6W provides the expected performance with an output

voltage of nearly 45V, considering the drop across the components. The overall analysis confirms that the proposed converter is suitable for medium voltage boosting applications such as renewable energy, microgrid, and uninterruptible power supplies (UPS).

REFERENCES

- [1]. Ling Qin, Lei Zhou, Waqas Hassan, John Long Soon, Min Tian and Jiapeng Shen, "A Family of Transformer-Less Single-Switch Dual- Inductor High Voltage Gain Boost Converters with Reduced Voltage and Current Stresses, ", IEEE Transactions on Power Electronics, Vol. 36, No. 5, May 2021
- [2]. Zahra Saadatizadeh, Pedram Chavoshpour Heris, Mehran Sabahi, Ebrahim Babaei, "A DC-DC transformerless high voltage gain converter with low voltage stresses on switches and diodes", IEEE Transactions on Power Electronics, ,vol. 34, no. 11, pp. 10600-10609, Nov. 2019
- [3]. Yun Zhang, Lei Zhou, Mark Sumner, Ping Wang, Single-switch, wide voltage-gain range, boost DC-DC converter for fuel cell vehicles, IEEE Transactions on Vehicle Technology, , vol. 67, no. 1, pp. 134-145, Jan. 2018
- [4]. Moumita Das, Vivek Agarwal, Design and analysis of a high-efficiency DC-DC converter with soft capability for renewable energy applications requiring high voltage gain, IEEE Transactions on Industrial Electronics,, vol. 63, no. 5, pp. 2936-2944, May. 2016.
- [5]. Si Chen, Luwei Zhou, Quanming Luo, Wei Gao, Yuqi Wei, Pengju Sun, Xiong Du, Research on topology of the high step-up boost converter with coupled Inductor, IEEE Transactions on Power Electronics, vol. 34, no. 11, pp. 10733-10745, Nov. 2019.
- [6]. Dongsheng Yu, Jie Yang, Ruidong Xu, Zhenglong Xia, Herbert HoChing Iu, Tyrone Fernando, A family of module-integrated high step-up converters with dual coupled inductors, IEEE Access,, vol. 6, pp. 16256-16266, Apr. 2018.
- [7]. Mojtaba Forouzesh, Yam P. Siwakoti, Saman A. Gorji, Frede Blaabjerg, Brad Lehman, Step-Up DCDC Converters: A Comprehensive Review of Voltage Boosting Techniques, Topologies, and Applications, IEEE Transactions on Power Electronics,, vol. 32, no. 12, December 2017.
- [8]. Zhilei Yao, "A Doubly Grounded Transformerless PV Grid-Connected Inverter Without Shoot-Through Problem ," IEEE Transactions on Industrial Electronics, 2020
- [9]. Abdul Fathah, Design of a Boost Converter, Department of Electrical Engineering, National Institute of Technology, Rourkela-769008(ODISHA)